

High-dose etoposide formulations do not saturate intestinal P-glycoprotein

Development, stability, and pharmacokinetics in Sprague-Dawley rats

Al-Ali, Ahmed A. Abdulhussein; Sandra, Louis; Versweyveld, Dries; Pijpers, IJs; Dillen, Lieve; Vermeulen, An; Snoeys, Jan; Holm, René; Nielsen, Carsten Uhd

Published in:
International Journal of Pharmaceutics

DOI:
[10.1016/j.ijpharm.2020.119399](https://doi.org/10.1016/j.ijpharm.2020.119399)

Publication date:
2020

Document Version
Peer reviewed version

Citation for published version (APA):
Al-Ali, A. A. A., Sandra, L., Versweyveld, D., Pijpers, I., Dillen, L., Vermeulen, A., Snoeys, J., Holm, R., & Nielsen, C. U. (2020). High-dose etoposide formulations do not saturate intestinal P-glycoprotein: Development, stability, and pharmacokinetics in Sprague-Dawley rats. *International Journal of Pharmaceutics*, 583, Article 119399. <https://doi.org/10.1016/j.ijpharm.2020.119399>

General rights

Copyright and moral rights for the publications made accessible in the public portal are retained by the authors and/or other copyright owners and it is a condition of accessing publications that users recognise and abide by the legal requirements associated with these rights.

- Users may download and print one copy of any publication from the public portal for the purpose of private study or research.
- You may not further distribute the material or use it for any profit-making activity or commercial gain.
- You may freely distribute the URL identifying the publication in the public portal.

Take down policy

If you believe that this document breaches copyright please contact rucforsk@kb.dk providing details, and we will remove access to the work immediately and investigate your claim.

**High-dose etoposide formulations do not saturate intestinal P-glycoprotein: Development,
stability, and pharmacokinetics in Sprague-Dawley rats**

**Ahmed A. Abdulhussein Al-Ali^a, Louis Sandra^b, Dries Versweyveld^c, Ils Pijpers^d, Lieve Dillen^d,
An Vermeulen^b, Jan Snoeys^d, René Holm^{e,f}, and Carsten Uhd Nielsen^{a*}**

^a: Department of Physics, Chemistry and Pharmacy, University of Southern Denmark, Campusvej 55,
DK-5230 Odense M, Denmark

^b: Quantitative Sciences, Janssen R&D, a division of Janssen Pharmaceutica NV, Turnhoutseweg 30,
2340 Beerse, Belgium

^c: Non Clinical Safety, Janssen R&D, a division of Janssen Pharmaceutica NV, Turnhoutseweg 30,
2340 Beerse, Belgium

^d: Drug Metabolism and Pharmacokinetics (DMPK), Janssen R&D, a division of Janssen
Pharmaceutica NV, Turnhoutseweg 30, 2340 Beerse, Belgium

^e: Drug Product Development, Janssen R&D, a division of Janssen Pharmaceutica NV,
Turnhoutseweg 30, 2340 Beerse, Belgium

^f: Department of Science and Environment, Roskilde University, 4000 Roskilde, Denmark

*: Corresponding author at: Department of Physics, Chemistry and Pharmacy, University of Southern
Denmark, Campusvej 55, DK-5230 Odense M, Denmark. Phone: +45 6550 9427 e-mail: cun@sdu.dk

21 **Abstract:** It has been suggested that oral absorption of low-permeable P-glycoprotein (P-gp)
22 substrates can be increased through saturation of P-gp. For BCS class IV drug substances, saturating
23 P-gp is challenging due to low aqueous solubility. The present study investigated if the BCS IV drug
24 substance etoposide could be solubilized to a concentration saturating P-gp after oral administration.
25 A formulation consisting of 10% (w/v) of pluronic® F-127 and polyvinylpyrrolidone/vinyl acetate
26 (PVP/VA), and 57% (v/v) ethanol enhanced etoposide's solubility approximately 100 times (16 mg
27 mL⁻¹) compared to its aqueous solubility. *In vitro*, this formulation was stable upon dilution in
28 simulated intestinal fluid. In male Sprague-Dawley rats, oral administration of increasing solubilized
29 etoposide doses using the formulation matrix increased the AUC_{0-∞} of etoposide dose-proportionally
30 but resulted in a lower absolute oral bioavailability (F) and rate of absorption as compared to control.
31 At the highest investigated dose (100 mg kg⁻¹), AUC_{0-∞} and C_{max} were significantly increased by 2.9-
32 and 1.4-fold, respectively, compared to control dosed at 20 mg kg⁻¹. A single oral dose of 20 mg kg⁻¹
33 zosuquidar followed by 20 mg kg⁻¹ oral etoposide increased F 8.6-fold. In conclusion, a stable
34 formulation with improved etoposide solubility was developed, yet the formulation did not result in
35 increased oral bioavailability of etoposide.

36

37 **Keywords:** P-glycoprotein, Etoposide, Zosuquidar, Population pharmacokinetics, Sprague-Dawley
38 rats.

39

40

41

42

43 **1. Introduction:**

44 P-glycoprotein (P-gp, MDR1) has been shown to limit the intestinal absorptive permeability of low-
45 permeable substrates in cell cultures (Alsenz et al., 1998; Collett et al., 1999; Sparreboom et al., 1997;
46 Terao et al., 1996; Troutman and Thakker, 2003b). *In vivo*, in wild type (WT) rats, P-gp restricts the
47 oral bioavailability of several P-gp substrates such as loperamide (Zamek-Gliszczynski et al., 2012),
48 paclitaxel (Zamek-Gliszczynski et al., 2012), digoxin (Nielsen et al., 2016), and etoposide (Al-Ali et
49 al., 2018a). This is evident since the oral bioavailability is significantly increased in *mdr1a* deficient
50 rats (Al-Ali et al., 2018a; Nielsen et al., 2016; Zamek-Gliszczynski et al., 2012). Moreover, co-
51 administration of P-gp substrates with potent small-molecular P-gp inhibitors such as verapamil
52 (Tsuruo et al., 1981), dexverapamil (Gramatté and Oertel, 1999), valspodar (PSC-833) (Mayer et al.,
53 1997; vanAsperen et al., 1997), or zosuquidar (LY335979) (Bardelmeijer et al., 2004) increased the
54 oral bioavailability of the substrates in preclinical studies. However, using inhibitors to increase the
55 oral bioavailability of P-gp substrates in some cases also affects metabolism via the cytochrome
56 P450s and results in adverse effects (Breedveld et al., 2006; Palmeira et al., 2012; Varma et al., 2003;
57 Varma and Panchagnula, 2005). Other studies have shown that co-administration of pharmaceutical
58 excipients such as nonionic surfactants may also have the potential to increase the oral bioavailability
59 of digoxin (Cornaire et al., 2004; Nielsen et al., 2016; Zhang et al., 2003), etoposide (Akhtar et al.,
60 2017; Al-Ali et al., 2018a), and paclitaxel (Varma and Panchagnula, 2005) in WT rats. To overcome
61 the cellular efflux mediated by P-gp to increase intestinal absorption, it should in theory be possible
62 to saturate the transporters by achieving intestinal concentrations well above the K_m -value for the
63 substrate-transporter binding as mentioned by e.g. Lin and Yamazaki (Lin and Yamazaki, 2003).
64 Taking into consideration the degree of passive diffusion, intestinal metabolism, and P-gp substrate
65 binding affinity, this may be a feasible strategy for drug substances with sufficient aqueous solubility,
66 low passive diffusion, and limited metabolism. The experimental evidence for the feasibility of

67 saturating P-gp in the intestine through a pharmaceutical formulation strategy is however relatively
68 limited and ambiguous. Lin and Yamazaki and Chiou et al., retrospectively, interpreted the
69 pharmacokinetic human studies of the BCS II compound talinolol made by de Mey et al., and
70 concluded that since the dose normalized AUC values after oral administration of increasing talinolol
71 doses increased with higher doses, this suggested saturation of P-gp efflux (Chiou et al., 2001; de
72 Mey et al., 1995; Lin and Yamazaki, 2003). Talinolol is also a substrate of absorptive solute carriers
73 including organic anion transporting polypeptide 1A2 (OATP1A2) and OATP2B1 (Shirasaka et al.,
74 2010) making the absorption kinetics quite complicated.

75 Since high doses of a P-gp substrate are needed to saturate the transporter, and as most P-gp substrates
76 are poorly water-soluble substances (Wang et al., 2001), suitable pharmaceutical formulation
77 approaches are required to solubilize the substrate. SMEEDs formulations could be used, but they
78 often contain surfactants that are also P-gp inhibitors see e.g. Zhao et al. (Zhao et al., 2013). Thus, in
79 the present study a formulation that can maintain the substrate in a solubilized-form upon dilution in
80 the intestinal lumen without P-gp inhibiting surfactants was developed using etoposide a BCS class
81 IV P-gp substrate. Etoposide was selected since intestinal P-gp limited oral etoposide bioavailability
82 in WT rats, whereas etoposide was completely absorbed in *mdr1a* deficient rats (Al-Ali et al., 2018a).
83 Moreover, data suggests that Bcrp has very little impact on the intestinal absorption of etoposide in
84 mice (Allen et al., 2003). A formulation was designed with ethanol and surfactant to enhance the
85 solubility of etoposide. Etoposide has a low aqueous solubility of 0.15-0.2 mg mL⁻¹ (Beig et al., 2015;
86 Darwish et al., 1989) and since 10% ethanol significantly enhanced etoposide stability in artificial
87 intestinal fluid, ethanol was used as a solubilizing co-solvent for etoposide (Joel et al., 1995). Since
88 many nonionic surfactants inhibit P-gp *in vitro* (Al-Ali et al., 2019; Al-Ali et al., 2018b; Batrakova
89 et al., 1999; Batrakova et al., 2003; Gurjar et al., 2018; Li-Blatter et al., 2012; Lo, 2003; Zhao et al.,
90 2016) and *in vivo* (Akhtar et al., 2017; Al-Ali et al., 2018a; Ma et al., 2011; Nielsen et al., 2016; Zhao

et al., 2013), a surfactant without P-gp inhibiting properties was chosen to evaluate the effect of increasing the dose of etoposide without a potential surfactant mediated P-gp inhibitory effect. Previous *in vitro* studies have reported that pluronic® F-127 did not inhibit the P-gp-mediated efflux of several substrates e.g. rhodamine 123 (Al-Ali et al., 2019; Batrakova et al., 2003; Wei et al., 2013), nelfinavir (Shaik et al., 2008), digoxin (Gurjar et al., 2018), and etoposide (Al-Ali et al., 2018a), hence this surfactant was chosen. Polyvinylpyrrolidone-vinyl acetate (PVP/VA) was suggested as a potential precipitation inhibitor (Kalaiselvan et al., 2006; Knopp et al., 2016; Xu and Dai, 2013) and formulation stabilizer during storage (Knopp et al., 2016; Prudic et al., 2014), thus it was included in the formulation.

The aim of the present study was to prepare an oral formulation of high concentration of etoposide and to investigate the stability on storage, and upon dilution in fasted state simulated intestinal fluid (FaSSIF). Furthermore, the formulation was used to investigate if the systemic exposure of orally administered etoposide in rats could be increased through saturation of P-gp transport activity.

104

2. Material and methods:

2.1. Materials

Caco-2 cells were obtained from the American Type Culture Collection (ATCC). Cell culture media and Hanks balanced salt solution (HBSS) were obtained from Life Technologies (Høje-Taastrup, Denmark). Etoposide (>99% purity) was purchased from Selleckchem (Munich, Germany). Sodium chloride, sodium taurocholate, sodium hydroxide, potassium chloride, L- α -phosphatidylcholine (approx. 60%), potassium phosphate monobasic ($\geq 97\%$), and pluronic® F-127 suitable for cell culture, 2-(N-morpholino) ethane sulfonic acid (MES), N-[2-Hydroxyethyl] piperazine N'-[2-ethanesulfonate] (HEPES), verapamil, digoxin, and bovine serum albumin (BSA) were from Sigma

114 (Brøndby, Denmark). Ethanol (99.5 %) was from VWR Chemicals (Fontenay-sous-Bois, France).
115 Polyvinylpyrrolidone-vinyl acetate (Kollidon[®] VA 64, referred as PVP/VA) meets Ph. Eur. standards
116 and was from BASF SE (Ludwigshafen, Germany). Transwell[®] inserts with polycarbonate membrane
117 (0.4 μm pore size, 1.12 cm^2) were from Corning Life Sciences and purchased through Sigma Aldrich
118 (Brøndby, Denmark). Whatman[®] Nuclepore[™] Track-Etched Membranes (0.03 μm pore-size, 19 mm
119 in diameter) were purchased from Sigma Aldrich (Brøndby, Denmark). LOCTITE[®] 401 glue was
120 purchased from RS Components Ltd. (Corby, UK). ³H-etoposide (specific activity 700 mCi mmol⁻¹)
121 was from Moravek (CA, USA). ¹⁴C-glycine (specific activity 87 mCi mmol⁻¹) was purchased from
122 Larodan (Solna, Sweden) and ¹⁴C-mannitol with a specific activity of 51.50 mCi/mmol was from
123 Sigma Aldrich (Brøndby, Denmark). Ultima Gold liquid was purchased from Perkin Elmer
124 (Skovlunde, Denmark). The radio-chemical purity of the isotopes was greater than 97%.

125

126 2.2. Cell culture and transport experiments

127 Caco-2 cells were cultured as previously described by Nielsen and co-workers (Nielsen et al., 2001).
128 Briefly, cells were seeded in culture flasks and passaged in Dulbecco's Modified Eagle's medium
129 (DMEM) supplemented with 10 % fetal bovine serum, penicillin/streptomycin (100 U ml⁻¹ and 100
130 $\mu\text{g ml}^{-1}$, respectively), 1 % L-glutamine, and 1 % non-essential amino acids. Cells were seeded onto
131 tissue culture treated Transwells (1.0 cm^2 , 0.4 μm pore size) at a density of 10⁵ cells cm^{-2} .
132 Transepithelial electrical resistance (TEER) at room temperature was measured before the
133 experiment. All TEER values of monolayers used were >400 $\Omega \text{ cm}^2$. Transport experiments were
134 performed on day 24-28 after seeding.

135 Apical (A) to basolateral (B) and B to A fluxes of tritium labeled etoposide was measured in 10 mM
136 HEPES buffers adjusted to pH 7.4. The concentration of etoposide on the donor (cis) side was 20 –

137 520 μM . Samples (20 μl) were taken from the donor solution at $t=0$ and 210 min and 150 μl samples
138 were taken from the receiver solution and replaced with fresh buffer ($t=30, 60, 90, 120, 150, 180$, and
139 210 min). The transport of ^3H -etoposide was also measured in the presence of 100 μM of digoxin and
140 50 μM verapamil on both donor and receiver side, respectively. Samples were transferred to
141 scintillation vials, where 2 ml of scintillation fluid was added and the radioactivity was counted in a
142 liquid scintillation analyzer. Fluxes were constant after 60 min. The steady state flux values were thus
143 obtained as the means of the flux values between 90-210 min. After the experiment, the integrity of
144 the Caco-2 cell monolayers was evaluated by ^{14}C -mannitol transport studies. Samples were taken
145 from the donor chamber (10 μl) at 20, 40, and 60 min, and from the receiver chamber at 0, 20, 40,
146 and 60 min. The permeability (P_{app}) of mannitol was unaffected by etoposide, digoxin and verapamil
147 and had a P_{app} value of $1.4 \cdot 10^{-06} \pm 4.2 \cdot 10^{-07} \text{ cm s}^{-1}$. The transport across the filter without Caco-2 cells
148 was investigated in order to assess whether the filter was a barrier to diffusion of etoposide. The
149 permeability across the filter was calculated using non-steady state kinetics and had a value of $3.1 \cdot 10^{-04} \pm 4.2 \cdot 10^{-05} \text{ cm s}^{-1}$.
150

151 The P-gp dependent flux ($J_{\text{P-gp}}$) was calculated similarly to described by Troutman and Thakker
152 (Troutman and Thakker, 2003a), where the total flux of etoposide was subtracted with the flux of
153 etoposide in the presence of 100 μM of digoxin and 50 μM verapamil to yield the concentration
154 dependent effect of P-gp on etoposide transport. Here we used Caco-2 cells from ATCC, and
155 proteomics data suggest that BCRP expression is very low in the substrain compared to Caco-2 cells
156 obtained from The European Collection of Authenticated Cell Cultures (ECACC) or/and Deutsche
157 Sammlung von Mikroorganismen und Zellkulturen (DSMZ), as reviewed in Al-Ali et al., 2019 (Al-
158 Ali et al., 2019). In Caco-2 cells from DSMZ it has been shown that 25 μM zosuquidar abolish
159 polarized etoposide transport completely (Nielsen et al., 2020), while it has also been shown that

160 verapamil completely abolishes polarized etoposide in Caco-2 cells (Mo et al., 2011). Therefore, it
161 seems likely that in Caco-2 cells from ATCC BCRP has a minor impact on etoposide transport.
162 The resulting etoposide flux in the B-A direction was then fitted to the following equation:

163

164
$$J_{P-gp} = \frac{J_{P-gp,max} * C_d}{K_{m,app} + C_d} \quad (1)$$

165 where, J_{P-gp} is the P-gp mediated flux, $J_{P-gp,max}$ is the maximal flux, $K_{m,app}$ is the apparent Michaelis
166 constant and C_d is the donor concentration.

167

168 2.3. Animals

169 *In vivo* pharmacokinetic studies were performed in WT male Sprague-Dawley rats, which were from
170 Charles River Laboratories (Sulzfeld, Germany). The study protocol was approved by the local ethical
171 committee in accordance with EC Directive 2010/63/EU and Belgian Law/1991 for Protection of
172 Vertebrate Animals used for Experimental and other Scientific Purposes. The rats were received one
173 week prior to the *in vivo* experiments, acclimatized and maintained on standard feed conditions with
174 free access to water. The animals were fasted for 16 h before the pharmacokinetic studies. During the
175 experiments, the rats had free access to water, but not food. At the day of the experiment, the weight
176 of the animals was 242-275 g.

177

178 2.4. Preparation of etoposide-containing formulations

179 Different formulations of etoposide were prepared using the nonionic surfactant pluronic® F-127, the
180 copolymer PVP/VA, ethanol, and ultra-purified water (Table 1). Pluronic® F-127 was first dissolved
181 in 57% (v/v) ethanol solution at room temperature. Etoposide was then added to the surfactant-

182 containing solution and placed in a water bath at 40° C for 15-30 min, before the solution was mixed
183 using a magnetic stirrer for 15-30 min. The solution was visually inspected for undissolved particles.
184 PVP/VA powder was subsequently added, and the mixture placed in a water bath at 37° C for 15-30
185 min, before being mixed using a magnetic stirrer for 15-30 min. The solution was again visually
186 investigated for undissolved particles. Finally, provided that the etoposide-containing formulation
187 was clear, the formulation was transferred to a glass container, protected from light, and kept at room
188 temperature overnight (approx. 15 h). If no sign of precipitation appeared after 15 h, the formulation
189 was further investigated for precipitation upon dilution with FaSSIF, see details below.

190

191 *2.5. Monitoring of etoposide containing-formulations diluted with fasted state simulated*
192 *intestinal fluid*

193 Monitoring that etoposide does not precipitate in the different formulations when diluted with FaSSIF
194 was investigated as previously described by Al-Ali et al. (Al-Ali et al., 2018a). Briefly, FaSSIF was
195 prepared according to Galia et al., composed of 0.39 g potassium phosphate monobasic, 0.77 g
196 potassium chloride, 3 mM sodium taurocholate, 0.75 mM L- α -phosphatidylcholine, and ultra-purified
197 water added to 100 mL (Galia et al., 1998). The pH was then adjusted to 6.50 ± 0.05 with sodium
198 hydroxide before the osmolality was adjusted to 270 ± 10 mOsm kg⁻¹ using sodium chloride (Galia
199 et al., 1998). The different formulations of etoposide were then added to FaSSIF in a ratio of 1:2
200 (formulation:FaSSIF) to simulate the likely intestinal dilution in the rats (McConnell et al., 2008) and
201 monitored for two hours by measuring the absorbance at 400 nm and 25° C every 10 min using a UV-
202 spectrophotometer (Genesys 10-S from Thermo Fisher Scientific (WI, USA)). Before each
203 measurement, solutions were mixed for 10 seconds using pipetting.

204

2.6. Dialysis studies investigating etoposide release from different formulations

Dialysis studies were designed and optimized as previously described by Al-Ali et al. (Al-Ali et al., 2018a), with minor modifications. In brief, the dialysis setup allows the diffusion of free-fraction of etoposide (unbound to micelles) and retains etoposide-bound to micelles, which should be not diffused across a 0.03 μm pore-size polycarbonate membrane during the course of the experiment (2 h). Polycarbonate membranes (0.03 μm pore size, 19 mm in diameter) were attached to Transwell holders (1.12 cm^2) by LOCTITE® 401 glue and left to dry at room temperature overnight (Al-Ali et al., 2018a). The Transwell inserts, with attached polycarbonate membranes, were then hydrated overnight in ultra-purified water. On the day of the experiment, Transwell inserts with polycarbonate membranes were first pre-incubated with HBSS supplemented with 10 mM HEPES and adjusted to pH 7.40 ± 0.05 (HBSS⁺) on a shaking plate at 220 rpm at 37° C for 10 min. Donor solutions of ³H-etoposide and ¹⁴C-glycine were prepared in HBSS⁺ (Control), or in different formulation-matrices containing 10% (w/v) PVP/VA, 57% (v/v) ethanol, and pluronic® F-127 at 1.5, 3 or 10%, referred to as Matrix-PF127 1.5%, Matrix-PF127 3%, or Matrix-PF127 10%, respectively, or mixed with a formulation with the highest concentration of etoposide. This formulation contained 15-16 mg mL^{-1} etoposide, 10% (w/v) of pluronic® F-127 and PVP/VA, and 57% (v/v) ethanol. The solution containing radioactive compounds was then added to FaSSIF at a 1:2 ratio to achieve final concentrations of ³H-etoposide and ¹⁴C-glycine at 0.25 $\mu\text{Ci mL}^{-1}$, 0.36 μM and 0.25 $\mu\text{Ci mL}^{-1}$, 2.87 μM , respectively, before these isotopes-containing solutions (500 μL) were added to the upper side of the polycarbonate membrane. Experiments started when receiver-release media (1650 μL) was loaded in the lower side of the polycarbonate membrane. Receiver-release media consisted of HBSS buffer supplemented with 10 mM HEPES and adjusted to pH 6.50 ± 0.05 for all conditions except for the formulation containing the highest concentration of etoposide where the medium was the matrix of this formulation (i.e. 10% of pluronic® F-127 and PVP/VA, and 57% ethanol without

etoposide) in order to prevent etoposide precipitation when accumulated in the receiver chamber. Experiments were performed at 37° C and shaking mode 220 rpm. Donor samples were collected at 0, 60 and 120 min, while receiver samples were collected at 15, 30, 60, 90, and 120 min. Receiver-release medium was replaced at each sampling occasion in order to preserve the sink condition. Finally, Ultima Gold scintillation fluid (2 mL) was added to every sample, vortexed for one minute and counted for 10 min on a scintillation counter (TriCarb 4910TR) from Perkin Elmer, USA.

235

2.7. Pharmacokinetic study in wild-type male Sprague-Dawley rats

The rats were randomly assigned to receive different doses of etoposide in ethanol solution or in a formulation matrix consisting of 10% (w/v) pluronic® F-127 and PVP/VA, 57% (v/v) ethanol, and ultra-purified water. For intravenous administration, the rats received etoposide solution (2.86 mg mL⁻¹ in 57% v/v ethanol) at a dose of 5 mg kg⁻¹ etoposide. Administration volume was adjusted to 2 mL with water before dosing the rats. For oral administration by oral gavage, the control group received an etoposide solution (2.86 mg mL⁻¹ in 57% v/v ethanol) at a dose of 20 mg kg⁻¹ etoposide and a dosing volume of 7 mL kg⁻¹. In the positive control group, the rats received a zosuquidar solution (2 mg mL⁻¹) at a dose of 20 mg kg⁻¹ and dosing volume of 10 mL kg⁻¹, 30 min before the administration of etoposide doses which were administered in a similar fashion to the control group. For oral administration of increasing doses of etoposide, an increasing concentration of etoposide was solubilized in the formulation matrix i.e. 2.86, 7.15 and 14.3 mg mL⁻¹. These etoposide-containing formulations were administered at doses of 20, 50, and 100 mg kg⁻¹, respectively, in a dosing volume of 7 mL kg⁻¹. Each dosing group consisted of 5-6 male Sprague-Dawley rats. After oral or intravenous administration of etoposide, blood samples were collected at 0.25, 0.5, 0.75, 1, 2, 3, 4, and 6 h, as well as at 5 min (0.0833 h) post intravenous administration of etoposide. The samples were obtained

252 at each sampling point by puncturing the lateral tail vein using a 23G needle and approximately 35
253 μ L of blood were collected using a capillary tube from VITREX Medical A/S (Herlev, Denmark).
254 The capillaries with samples were then sealed with VITREX Sigillum Wax. Plasma samples were
255 harvested immediately from these capillaries after centrifugation at 1900xg for 10 min at 4° C and
256 transferred to a 10 μ L end-to-end capillary (VITREX) followed by storage at -20° C until further
257 bioanalysis. At 6 h, the last samples were collected, and the animals were euthanized.

258

259 2.8. *Quantification of etoposide in pharmacokinetic studies*

260 Quantification of etoposide in plasma samples was performed on an API 4000™ LC/MSMS System
261 from AB SCIEX (Ontario, Canada). Briefly, plasma samples were precipitated with acetonitrile after
262 wash-out from the end-to-end capillaries. Chromatographic separation was carried out using an
263 Acquity UPLC BEH C18 column (1.7 μ m, 2.1 mm \times 50 mm). Gradient elution was performed at 50
264 °C with 0.01M ammonium acetate (mobile phase A) and acetonitrile (mobile phase B). Starting
265 conditions were 5 % B for 0.25 minutes, then a linear gradient to 95% B was applied over 1.25
266 minutes, followed by an isocratic hold at 95% B for 0.5 min before re-equilibration at 5% B. Total
267 run time was 2.5 min and a flow rate of 0.6 mL/min was applied.

268 The LC-MS/MS was operated in positive ion mode using the TurboIonSpray™-interface
269 (electrospray ionization), and was optimized for the quantification of etoposide, applying multiple
270 reaction monitoring (m/z 587.2 \rightarrow m/z 381).

271 Incurred samples were quantified against calibration curves prepared in blank rat plasma. Independent
272 quality control samples were included to evaluate accuracy (between 80 and 120% of the nominal

value) of the analytical run. The concentrations were correlated linearly, with a $1/x^2$ weighing, with the MS response between 1.00 and 10000 ng mL⁻¹.

275

2.9. Population Pharmacokinetic analysis

Population pharmacokinetic analysis was performed using Monolix 2018R2 (Lixoft SAS, Antony, France) based on a two-compartment population pharmacokinetic model with linear first order elimination and an oral depot compartment with subsequent first order absorption. Population pharmacokinetic parameter estimates were generated using the stochastic approximation expectation-maximization (SAEM) algorithm. Modeling was performed using the clearance parameterization assuming a lognormal distribution of individual parameters. The individual parameter estimates for the i th subject were modeled according to equation 2.

$$\theta_i = \theta_{pop} \cdot e^{\eta_{\theta,i}} \quad (2)$$

where θ_i is the individual parameter estimate for the i th subject, θ_{pop} is the typical population parameter estimate and $\eta_{\theta,i}$ is assumed to be the random individual deviation for the i th subject for a particular population parameter θ . The clearance parametrization included the volume of the central compartment (V_1), the elimination clearance (CL), the volume of the peripheral compartment (V_2), and the inter-compartmental flow between the central and the peripheral compartment (Q_2). Oral administration was modeled using a dosing compartment and subsequent first order absorption. The final model included covariate effects, which partly explained differences observed between animals assigned to the different formulation groups. Forward inclusion of covariates was judged based on the decrease in objective function value expressed as -2 log likelihood (-2LL) and Akaike's information criterion (AIC). Covariate selection was guided by physiological plausibility and

295 statistical significance ($P < 0.05$). Covariate effects of the final population model included the
 296 presence of zosuquidar on F and the presence of experimental matrix (referred as formulation G-
 297 matrix) on F and k_a . The final model estimated inter-individual variability for F, k_a , V_1 and CL.
 298 Residual error was accounted for by a combined (additive and proportional) error model (Equation
 299 3).

$$300 \quad \log(Y_{ij}) = \log(c_{\text{pred},ij}) + (a + b \cdot \log(c_{\text{pred},ij}))\epsilon_{ij} \quad (3)$$

301 where the j th observation of the i th subject deviates from the j th prediction of the i th subject, $c_{\text{pred},ij}$,
 302 by an additive term, a , and a proportional term, b . ϵ_{ij} was assumed to be the random variable for the
 303 j th concentration of the i th individual, sampled from a distribution with zero as a mean and a variance
 304 of σ^2 . Individual Bayesian estimates were used to calculate mean $\text{AUC}_{0-\infty}$ per study cohort. Individual
 305 $\text{AUC}_{0-\infty}$ values ($\text{AUC}_{0-\infty,i}$) were calculated as shown in equation 4.

$$306 \quad \text{AUC}_{0-\infty,i} = \frac{F_i \cdot D}{\text{CL}_i} \quad (4)$$

307

308 2.10. Statistics

309 The results of *in vitro* studies were obtained from at least three experiments and presented as mean
 310 values \pm SEM. Caco-2 cell experiments were conducted in three independent cell passages and values
 311 are presented as mean values \pm SEM. The results of the *in vivo* pharmacokinetic studies were obtained
 312 from 5 or 6 rats per study cohort and data are presented as mean values \pm SEM. Statistical analysis
 313 was performed using GraphPad Prism 7.01 from GraphPad Software, LLC (San Diego, CA, USA).
 314 One-way ANOVA test followed by Tukey's multiple comparisons test were selected for multiple
 315 comparisons. P value < 0.05 was considered statistically significantly different from control.

Moreover, dose-proportionality has been assessed by plotting $AUC_{0-\infty}$ as a function of oral etoposide doses and linear regression analysis was performed.

3. Results

3.1. Transepithelial flux of etoposide across Caco-2 cells

Etoposide transport across Caco-2 monolayers was investigated, and in the following Figure 1, the A-B and B-A flux dependent on P-gp is shown. The A-B flux dependent on P-gp shows a gradual increase as a function of concentration and at higher concentrations the flux is relatively linear as a function of concentration in the apical donor solution (Fig. 1A). In the B-A direction, the flux of etoposide across Caco-2 cells monolayers can be described by Michaelis-Menten like kinetics where the flux becomes saturated with increasing concentration in the basolateral medium. The resulting kinetical parameters were estimated at $257 \pm 32 \mu\text{M}$, $199 \pm 17 \text{ pmol cm}^{-2} \text{ min}^{-1}$, and 1.7 ± 0.2 for $K_{m,app}$, $J_{P-gp, max}$, and the Hill coefficient, respectively.

3.2. Etoposide did not precipitate in formulations containing high percentages of ethanol

Different formulations of etoposide were prepared using 44% or 57% (v/v) ethanol, 2-10% (w/v) pluronic[®] F-127, and 0-15% (w/v) PVP/VA (Table 1). Etoposide in formulations containing 44% (v/v) ethanol either contained low concentration of etoposide such as 9 mg mL^{-1} (Formulation A), which was not sufficient to perform our study or precipitated after overnight incubation such as Formulation B (Fig. 2). Etoposide formulations (C-G) showed no signs of etoposide precipitation after overnight incubation; e.g. Formulation G as shown in Figure 2. Etoposide solubility in these formulations containing 57% (v/v) ethanol was higher than in formulation A and B. Formulation D showed that 6% (w/v) of the surfactant was required to dissolve 15 mg mL^{-1} etoposide in PVP/VA-

339 free formulation. Formulations A, C, and E-G were designed to contain 5-15% (w/v) PVP/VA as a
340 potential precipitation inhibitor. Formulation G consisting of 10% (w/v) of pluronic[®] F-127 and
341 PVP/VA, 57% ethanol, and water could solubilize an amount of etoposide corresponding to a 100-
342 fold increase compared to the aqueous solubility. Further studies were conducted to investigate
343 whether etoposide precipitates after the addition of different formulations to FaSSIF.

344

345 *3.3. Etoposide did not precipitate from Formulation G after dilution in fasted state simulated*
346 *intestinal fluid*

347 Formulations C-E showed a fast etoposide precipitation (less than 30 min) after dilution in FaSSIF.
348 Formulation F started to precipitate after approx. one hour and reached similar levels of absorbance
349 values as C-E at 90 min. Therefore, formulations C-F were only prepared and investigated once.
350 Formulation G showed no sign of etoposide precipitation for 120 min (Fig. 3). After 120 min,
351 etoposide started to precipitate indicating that the matrix of formulation G was able to maintain
352 etoposide in a solubilized form in FaSSIF for two hours (Fig. 3), which is the period that likely covers
353 the absorption phase of etoposide in rats. Equal amounts of pluronic[®] F-127 and PVP/VA at 10%
354 (w/v) were required to maintain etoposide in a solubilized form when diluted with FaSSIF. Among
355 the investigated formulations, formulation G was stable in FaSSIF and the next step was to investigate
356 if the formulation G would retain etoposide.

357

358 *3.4. Etoposide release was similar from different surfactant-containing solutions and matrix of*
359 *formulation G*

360 As shown in Figure 4, simultaneous etoposide and glycine release from different pluronic® F-127-
361 containing solutions and formulation G to receiver-release media increased time dependently. The
362 release of etoposide and glycine from different pluronic® F-127-containing formulations and from
363 formulation G was similar to the release in the control buffer i.e. without surfactant. Moreover, there
364 was no statistically significant difference between the slopes of the time-dependent release of
365 etoposide or glycine compared to control. The presence of non-radiolabeled etoposide in formulation
366 G did not affect the release of radiolabeled etoposide during the course of the experiment.

367

368 *3.5. Etoposide population pharmacokinetics in WT male Sprague-Dawley rats after intravenous*
369 *and oral administration*

370 Pharmacokinetic data available included 321 concentration-time points collected from 35 male WT
371 Sprague-Dawley rats. The PK profile af intravenous administration of etoposide is shown in figure 5,
372 illustrating a fast distribution phase followed by a slower elimination phase. Data points at 4 h post
373 intravenous administration of etoposide are not shown in Figure 5 as the plasma concentration values
374 were below the limit of quantification (LOQ) at this time point, and only three plasma-concentrations
375 had values above LOQ at 6 h. Etoposide pharmacokinetic profiles after oral administration of
376 etoposide-containing solutions were best described by a two-compartment structural model with
377 linear elimination and first-order absorption (Fig. 6). Subsequently, a covariate model was developed
378 to account for the inter-individual variability arising from the experimental design. The introduction
379 of zosuquidar dose as a covariate on the oral bioavailability F, and matrix-G presence as a covariate
380 on F as well as on the absorption rate constant (k_a) significantly improved the model fit. After
381 covariate inclusion, the unexplained inter-individual variability for F and k_a , calculated as the square
382 root of the exponential variance of η minus 1, decreased from 153% for F and 59.7% for k_a to 15.9%

383 and 53.5%, respectively, from the base structural model to the final covariate model ($\Delta 138\%$ for F
384 and $\Delta 6.15\%$ for k_a). Estimated population pharmacokinetic parameters, precision of the parameter
385 estimates and objective function values of both the base structural model and the final covariate model
386 are presented in Table 2. Empirical Bayesian estimates were used to calculate $AUC_{0-\infty}$ and dose
387 normalized $AUC_{0-\infty}$. $AUC_{0-\infty}$, dose normalized $AUC_{0-\infty}$, $t_{1/2}$, t_{max} and C_{max} are presented in Table 3.
388 Rats pretreated with zosuquidar showed the largest etoposide exposure ($AUC_{0-\infty}$ of $4511 \text{ ng h mL}^{-1}$
389 kg). Dose-proportional etoposide exposure was observed for the 20, 50, and 100 mg kg^{-1} dosing
390 cohorts receiving etoposide prepared in the matrix of formulation G (i.e. 10% of pluronic® F-127 and
391 PVP/VA, 57% ethanol, and water), and R square was equal to 0.99 when the AUC was plotted as a
392 function of dose (supplementary figure S1). However, the F, k_a , $AUC_{0-\infty}$, and C_{max} were significantly
393 lower when the rats were dosed with etoposide 20 mg kg^{-1} dissolved in the matrix of formulation G
394 compared to the control group. Etoposide oral bioavailability significantly increased when the rats
395 were pretreated with zosuquidar. The oral pharmacokinetic profile showed that the oral absorption of
396 etoposide was slower in matrix-based formulations as was also apparent from the decreased k_a values.

397

398 4. Discussion

399 In the present study, a stable formulation containing high concentration of etoposide and ethanol
400 (57%) was developed using a surfactant without P-gp inhibiting properties. After oral administration
401 of etoposide in this formulation, no increased bioavailability related to P-gp saturation could be
402 shown, illustrating the practical difficulties in saturating P-gp mediated transport of low soluble drug
403 substances for increasing the oral absorption through a formulation approach.

404 To investigate if the transport of etoposide was saturable, we used the approach described by
405 Troutman and Thakker (Troutman and Thakker, 2003a), in which the net flux due to P-gp mediated

transport is estimated by subtracting the flux under P-gp inhibited conditions. We found that the B-A transport was saturable with kinetical parameters similar to the ones described by Troutman and Thakker in Caco-2 cells, for $K_{m,app}$ 257 vs. 461 μM , and for J_{max} 199 vs. 354 $\text{pmol cm}^{-2} \text{min}^{-1}$ (Troutman and Thakker, 2003a). Makhey et al. found a similar K_m value of 113 μM in Caco-2 cells and 94-119 μM in stripped rat intestinal tissue (Makhey et al., 1998). Troutman and Thakker estimated a higher K_m value of 1360 μM for the A-B transport direction (Troutman and Thakker, 2003a), however this value was outside the concentration range that could be investigated in our set-up. Even though the B-A transport appears saturable and while it is more difficult to be assessed from the A-B transport, studies in wild-type and knock-out rats clearly show that the apically located P-gp is highly attenuating the oral etoposide absorption (Al-Ali et al., 2018a). Considering the above mentioned K_m values, generally of approximately 100-500 μM , an intestinal concentration of 10 times these values would likely be required to fully saturate P-gp mediated transport by etoposide itself, corresponding to approximately 5000 μM for the worst case scenario. A solubility higher than that could be achieved with formulation G (16 mg mL^{-1} (27183 μM)) containing 10% of pluronic® F-127 and 10% PVP/VA. 16 mg mL^{-1} is approximately 100-fold higher than the aqueous solubility of etoposide (Beig et al., 2015; Darwish et al., 1989). Pluronic® F-127 forms micelles that have the capacity to solubilize lipophilic drug substances e.g. meso-tetraphenyl porphine (mTPP) (Sezgin et al., 2007), rofecoxib (Ahuja et al., 2007), ibuprofen (Wan et al., 2010), paclitaxel, and lapatinib (Kelishady et al., 2015). The reported critical micelle concentration (CMC) values of pluronic® F-127 were 1, 0.1, and 0.025% (w/v) at 25, 30, and 35°C (Alexandridis and Hatton, 1995), respectively. Etoposide in micelles could be retained from permeation and hence the oral absorption could be decreased, which has been reported with 25% polysorbate 20 (Al-Ali et al., 2018a). However, the presence of different concentrations of pluronic® F-127 did not affect the *in vitro* release of etoposide and glycine compared to the release from a surfactant-free formulation. Similarly, 1% (w/v) pluronic®

430 F-127, which is above the CMC value, did not affect the release of the lipophilic drug rofecoxib
431 (Ahuja et al., 2007) (Log P 2.56) (Chemicalize, 2018).

432 Previous pharmacokinetic studies in rats have shown that t_{\max} of etoposide exposure was between
433 0.25-1.75 h (Al-Ali et al., 2018a; Li et al., 2009; Zhao et al., 2013), therefore the formulation should
434 maintain etoposide in its solubilized form for two hours when diluted in FaSSIF. This period was
435 considered sufficient for further *in vivo* studies. In formulation G, solubilized etoposide did not
436 precipitate for two hours when diluted with FaSSIF. Thus, pluronic® F-127 probably had two
437 functions: i) enhanced the solubility of etoposide, and ii) decreased the precipitation rate of etoposide
438 as it was also suggested by (Li et al., 2012; Xu and Dai, 2013), thereby stabilizing the formulation in
439 FaSSIF. Importantly, it seems that a balance between pluronic® F-127 and PVP/VA concentrations
440 (i.e. 10% of each) in the formulation was needed to achieve these formulation characteristics. Thus,
441 if an intestinal dilution of 3-10 is expected after oral administration of a 16 mg mL⁻¹ etoposide
442 formulation, and initial estimated intestinal concentration of 2718 – 9061 µM could be obtained,
443 which could be able to saturate P-gp assuming that etoposide remains in solution.

444 In rats receiving 100 mg kg⁻¹ of etoposide in formulation G, a higher AUC_{0-∞} was obtained compared
445 to rats receiving 20 mg kg⁻¹ etoposide in a 57% ethanol solution. Even though the systemic exposure
446 of etoposide increased with higher doses, the absolute bioavailability decreased, and this does not
447 seem to involve P-gp saturation by etoposide as the absolute bioavailability should then increase.
448 However, zosuquidar enhanced the oral absorption and bioavailability of etoposide. Yet, in the
449 presence of 20 mg kg⁻¹ zosuquidar, only 34.5% of the etoposide dose reached the systemic circulation,
450 thus zosuquidar itself most likely did not cause full inhibition of intestinal P-gp.

451 Surprisingly, the absolute oral bioavailability of etoposide was low compared to our previous study
452 (Al-Ali et al., 2018a). Al-Ali and coworkers reported that the oral bioavailability of etoposide was 27

453 $\pm 5\%$ (Al-Ali et al., 2018a). Zhao and co-workers reported an oral bioavailability of etoposide of 25
454 $\pm 7\%$ in WT male Sprague-Dawley rats dosed with 12 mg kg^{-1} etoposide suspended (1.5 mg mL^{-1}) in
455 0.5% sodium carboxymethyl cellulose (Zhao et al., 2013). Li and co-workers reported an oral
456 bioavailability of $7.5 \pm 1.8\%$ in WT male Sprague-Dawley rats after oral administration of a 6 mg kg^{-1}
457 etoposide solution prepared as an injectable formulation (specific composition not specified) (Li et
458 al., 2009). In the present study, it was not clear why the oral bioavailability of etoposide was low in
459 the control group, however, besides the known variabilities observed between animal studies (Festing
460 and Altman, 2002), one could speculate that the 57% of ethanol could be the cause, since etoposide
461 could precipitate in the intestinal lumen. In the previous study by Al-Ali et al, the oral bioavailability
462 of etoposide (27%) was obtained after administration of 20 mg kg^{-1} in 40% ethanol (2 mg mL^{-1})
463 administered with a dosing volume of 10 mL kg^{-1} (Al-Ali et al., 2018a). In the present study an
464 etoposide solution (2.86 mg mL^{-1}) in 57% (v/v) ethanol at a dose of 20 mg kg^{-1} etoposide and a dosing
465 volume of 7 mL kg^{-1} was used, thus approximately similar absolute amounts of ethanol were
466 administered in the two studies, but the concentration of etoposide and the amount of water differ,
467 with concentration of etoposide in the previous study being lower and water amount higher. This
468 could affect the susceptibility of etoposide precipitation in the solution used here to be higher. Ethanol
469 is rapidly absorbed in rats with a t_{max} less than 60 min and 50% disappearance of ethanol from the
470 stomach after 60 min (Siegers et al., 1972). If etoposide has indeed precipitated, this could explain
471 the low bioavailability. Population analysis indicated that formulation G decreased both the oral
472 bioavailability and the absorption rate while a clear increase in oral bioavailability was quantified in
473 the presence of zosuquidar administration. Introduction of these covariate effects on the respective
474 parameters of the population pharmacokinetic model significantly decreased the objective function
475 values (OFVs) and improved the model fit upon inspection of diagnostic plots (see Table 2). It has
476 been described earlier that 25% (v/v) polysorbate 20 decreased etoposide oral absorption, when

477 similar doses of 20 mg kg⁻¹ of etoposide were co-administered in rats (Al-Ali et al., 2018a). In the
478 study reported by Al-Ali et al., dialysis experiments showed that polysorbate 20 at 25% (v/v)
479 abolished etoposide release across polycarbonate membranes (Al-Ali et al., 2018a). In contrast, the
480 present study showed that etoposide release from the matrix across polycarbonate membrane was not
481 affected by the presence of different components in the formulation such as pluronic® F-127. *In vivo*,
482 this points to an effect of the high ethanol concentration rather than incomplete release from colloidal
483 structures present in the intestinal lumen.

484

485 5. Conclusion

486 In conclusion, an oral formulation of high-concentration of etoposide, which maintained etoposide in
487 a solubilized form under short-term storage conditions and when diluted with simulated intestinal
488 fluid was developed. Administration of increasing etoposide doses using this formulation-matrix
489 enhanced the plasma exposure of etoposide dose-proportionally. However, the applied doses were
490 not able to saturate P-gp, and the absolute absorption fraction decreased as a function of increasing
491 dose. To saturate intestinal P-gp by etoposide in rats, oral formulations maintaining high
492 concentrations of etoposide in solution are needed, yet the present study is a starting point for
493 developing formulation approaches using other drug candidates aimed at increasing the oral
494 absorption of P-gp substrates and illustrates the difficulties in developing formulations aimed at
495 saturating intestinal P-gp transport.

496

497

498 **Author Contributions:** Conceptualization, AAAA, RH, and CUN; methodology, AAAA, AV, JS,
499 RH, and CUN; investigation, AAAA, DV, IP, and LD; resources, RH and CUN; writing—original

500 draft preparation, AAAA and CUN; writing—review and editing, AAAA, LS, LD, IP, AV, JS, RH,
501 and CUN; formal analysis, AAAA, LS, AV, and CUN; supervision, RH and CUN; project
502 administration, CUN.

503

504 **Funding:** This research did not receive any specific grant from funding agencies in the public,
505 commercial, or not-for-profit sectors.

506

507 **Acknowledgments:** We thank the staff at the animal facility at Janssen Pharmaceutica NV for help
508 with performing the animal study. Greet Janssen at the animal facility is thanked for assisting with
509 the *in vivo* study and preparing the samples for bioanalysis. We thank the staff at the Drug Product
510 Development, Developability, at Janssen Pharmaceutica NV. Special thanks go to Marc Du Jardin
511 and Kris Van Dijck for their help in the lab and logistic support.

512

513 **Declaration of interest:** The authors do not have any conflict of interest to report.

514

515 **References**

516 Ahuja, N., Katare, O.P., Singh, B., 2007. Studies on dissolution enhancement and mathematical modeling of
517 drug release of a poorly water-soluble drug using water-soluble carriers. *Eur. J. Pharm. Biopharm.* 65, 26-38.

518 Akhtar, N., Ahad, A., Khan, M.F., Allaham, A., Talegaonkar, S., 2017. The Ameliorated Pharmacokinetics
519 of VP-16 in Wistar Rats: A Possible Role of P-Glycoprotein Inhibition by Pharmaceutical Excipients. *Eur. J.*
520 *Drug Metab. Pharmacokinet.* 42, 191-199.

521 Al-Ali, A.A.A., Nielsen, R.B., Nielsen, C.U., Steffansen, B., Holm, R., 2019. Nonionic surfactants modulate
522 the transport activity of ATP-binding cassette (ABC) transporters and solute carriers (SLC): Relevance to
523 oral drug absorption. *Int. J. Pharm.* 566, 410-433.

524 Al-Ali, A.A.A., Quach, J.R.C., Bundgaard, C., Steffansen, B., Holm, R., Nielsen, C.U., 2018a. Polysorbate
525 20 alters the oral bioavailability of etoposide in wild type and *mdr1a* deficient Sprague-Dawley rats. *Int. J.*
526 *Pharm.* 543, 352-360.

527 Al-Ali, A.A.A., Steffansen, B., Holm, R., Nielsen, C.U., 2018b. Nonionic surfactants increase digoxin
528 absorption in Caco-2 and MDCKII MDR1 cells: Impact on P-glycoprotein inhibition, barrier function, and
529 repeated cellular exposure. *Int. J. Pharm.* 551, 270-280.

530 Alexandridis, P., Hatton, T.A., 1995. Poly (ethylene oxide) . poly (propylene oxide) . poly (ethylene oxide)
531 block copolymer surfactants in aqueous solutions and at interfaces: thermodynamics, structure, dynamics,
532 and modeling. *Colloids Surf. A Physicochem. Eng. Asp.* 96, 1-46.

533 Allen, J.D., Van Dort, S.C., Buitelaar, M., van Tellingen, O., Schinkel, A.H., 2003. Mouse breast cancer
534 resistance protein (Bcrp1/Abcg2) mediates etoposide resistance and transport, but etoposide oral availability
535 is limited primarily by P-glycoprotein. *Cancer Res.* 63, 1339-1344.

536 Alsenz, J., Steffen, H., Alex, R., 1998. Active Apical Secretory Efflux of the HIV Protease Inhibitors
537 Saquinavir and Ritonavir in Caco-2 Cell Monolayers. *Pharm. Res.* 15, 423-428.

538 Bardelmeijer, H.A., Ouwehand, M., Beijnen, J.H., Schellens, J.H.M., van Tellingen, O., 2004. Efficacy of
539 novel P-glycoprotein inhibitors to increase the oral uptake of paclitaxel in mice. *Invest. New Drugs* 22, 219-
540 229.

541 Batrakova, E., Lee, S., Li, S., Venne, A., Alakhov, V., Kabanov, A., 1999. Fundamental Relationships
542 Between the Composition of Pluronic Block Copolymers and Their Hypersensitization Effect in MDR
543 Cancer Cells. *Pharm. Res.* 16, 1373-1379.

544 Batrakova, E.V., Li, S., Alakhov, V.Y., Miller, D.W., Kabanov, A.V., 2003. Optimal structure requirements
545 for pluronic block copolymers in modifying P-glycoprotein drug efflux transporter activity in bovine brain
546 microvessel endothelial cells. *J. Pharmacol. Exp. Ther.* 304, 845-854.

547 Beig, A., Miller, J.M., Lindley, D., Carr, R.A., Zocharski, P., Agbaria, R., Dahan, A., 2015. Head-To-Head
548 Comparison of Different Solubility-Enabling Formulations of Etoposide and Their Consequent Solubility-
549 Permeability Interplay. *J. Pharm. Sci.* 104, 2941-2947.

550 Breedveld, P., Beijnen, J.H., Schellens, J.H.M., 2006. Use of P-glycoprotein and BCRP inhibitors to improve
551 oral bioavailability and CNS penetration of anticancer drugs. *Trends Pharmacol. Sci.* 27, 17-24.

552 Chemicalize, 2018. chemicalize.com (accessed 02.11.2018).

553 Chiou, W., Chung, S., Wu, T., Ma, C., 2001. A comprehensive account on the role of efflux transporters in
554 the gastrointestinal absorption of 13 commonly used substrate drugs in humans. *Int. J. Clin. Pharmacol. Ther.*
555 39, 93-101.

556 Collett, A., Higgs, N.B., Sims, E., Rowland, M., Warhurst, G., 1999. Modulation of the permeability of H-2
557 receptor antagonists cimetidine and ranitidine by P-glycoprotein in rat intestine and the human colonic cell
558 line Caco-2. *J. Pharmacol. Exp. Ther.* 288, 171-178.

559 Cornaire, G., Woodley, J., Hermann, P., Cloarec, A., Arellano, C., Houin, G., 2004. Impact of excipients on
560 the absorption of P-glycoprotein substrates in vitro and in vivo. *Int. J. Pharm.* 278, 119-131.

561 Darwish, I.A., Florence, A.T., Saleh, A.M., 1989. Effects of Hydrotropic Agents on the Solubility,
562 Precipitation, and Protein Binding of Etoposide. *J. Pharm. Sci.* 78, 577-581.

563 de Mey, C., Schroeter, V., Butzer, R., Jahn, P., Weisser, K., Wetterich, U., Terhaag, B., Mutschler, E.,
564 Spahn-Langguth, H., Palm, D., Belz, G.G., 1995. Dose-Effect and Kinetic-Dynamic Relationships of the (β -
565 Adrenoceptor Blocking Properties of Various Doses of Talinolol in Healthy Humans. *J. Cardiovasc.*
566 *Pharmacol.* 26, 879-888.

567 Festing, M.F.W., Altman, D.G., 2002. Guidelines for the Design and Statistical Analysis of Experiments
568 Using Laboratory Animals. *ILAR Journal* 43, 244-258.

569 Galia, E., Nicolaides, E., Hörter, D., Löbenberg, R., Reppas, C., Dressman, J.B., 1998. Evaluation of Various
570 Dissolution Media for Predicting In Vivo Performance of Class I and II Drugs. *Pharm. Res.* 15, 698-705.

571 Gramatté, T., Oertel, R., 1999. Intestinal secretion of intravenous talinolol is inhibited by luminal R-
572 verapamil. *Clin. Pharmacol. Ther.* 66, 239-245.

573 Gurjar, R., Chan, C., Curley, P., Sharp, J., Chiong, J., Rannard, S., Siccardi, M., Owen, A., 2018. Inhibitory
574 effects of commonly used excipients on P-glycoprotein in vitro. *Mol. Pharm.* 15, 4835-4842.

575 Joel, S.P., Clark, P.I., Slevin, M.L., 1995. Stability of the i.v. and oral formulations of etoposide in solution.
576 *Cancer Chemother. Pharmacol.* 37, 117-124.

577 Kalaiselvan, R., Mohanta, G.P., Manna, P.K., Manavalan, R., 2006. Inhibition of albendazole crystallization
578 in poly(vinylpyrrolidone) solid molecular dispersions. *Die Pharmazie* 61, 618.

579 Kelishady, P.D., Saadat, E., Ravar, F., Akbari, H., Dorkoosh, F., 2015. Pluronic F127 polymeric micelles for
580 co-delivery of paclitaxel and lapatinib against metastatic breast cancer: Preparation, optimization and in vitro
581 evaluation. *Pharm. Dev. Technol.* 20, 1009-1017.

582 Knopp, M.M., Nguyen, J.H., Mu, H., Langguth, P., Rades, T., Holm, R., 2016. Influence of Copolymer
583 Composition on In Vitro and In Vivo Performance of Celecoxib-PVP/VA Amorphous Solid Dispersions.
584 *The AAPS Journal* 18, 416-423.

585 Li-Blatter, X., Beck, A., Seelig, A., 2012. P-glycoprotein-ATPase modulation: the molecular mechanisms.
586 *Biophys. J.* 102, 1383-1393.

587 Li, C., Li, X., Choi, J.-S., 2009. Enhanced bioavailability of etoposide after oral or intravenous
588 administration of etoposide with kaempferol in rats. *Arch. Pharm. Res.* 32, 133-138.

589 Li, S., Pollock-Dove, C., Dong, L.C., Chen, J., Creasey, A.A., Dai, W.-G., 2012. Enhanced bioavailability of
 590 a poorly water-soluble weakly basic compound using a combination approach of solubilization agents and
 591 precipitation inhibitors: a case study. *Mol. Pharm.* 9, 1100-1108.

592 Lin, J.H., Yamazaki, M., 2003. Role of P-Glycoprotein in Pharmacokinetics: Clinical Implications. *Adis*
 593 *International*, Cham, pp. 59-98.

594 Lo, Y.-I., 2003. Relationships between the hydrophilic–lipophilic balance values of pharmaceutical
 595 excipients and their multidrug resistance modulating effect in Caco-2 cells and rat intestines. *J. Control.*
 596 *Release* 90, 37-48.

597 Ma, L., Wei, Y., Zhou, Y., Ma, X., Wu, X.a., 2011. Effects of Pluronic F68 and Labrasol on the intestinal
 598 absorption and pharmacokinetics of rifampicin in rats. *Arch. Pharm. Res.* 34, 1939-1943.

599 Makhey, V.D., Guo, A., Norris, D.A., Hu, P., Yan, J., Sinko, P.J., 1998. Characterization of the Regional
 600 Intestinal Kinetics of Drug Efflux in Rat and Human Intestine and in Caco-2 Cells. *Pharm. Res.* 15, 1160-
 601 1167.

602 Mayer, U., Wagenaar, E., Dorobek, B., Beijnen, J.H., Borst, P., Schinkel, A.H., 1997. Full blockade of
 603 intestinal P-glycoprotein and extensive inhibition of blood-brain barrier P-glycoprotein by oral treatment of
 604 mice with PSC833. *J. Clin. Invest.* 100, 2430-2436.

605 McConnell, E.L., Basit, A.W., Murdan, S., 2008. Measurements of rat and mouse gastrointestinal pH, fluid
 606 and lymphoid tissue, and implications for in-vivo experiments. *J. Pharm. Pharmacol.* 60, 63-70.

607 Mo, R., Xiao, Y., Sun, M., Zhang, C., Ping, Q.J.I.j.o.p., 2011. Enhancing effect of N-octyl-O-sulfate chitosan
 608 on etoposide absorption. *Int. J. Pharm.* 409, 38-45.

609 Nielsen, C.U., Abdulhussein, A.A., Colak, D., Holm, R., 2016. Polysorbate 20 increases oral absorption of
 610 digoxin in wild-type Sprague Dawley rats, but not in *mdr1a*(-/-) Sprague Dawley rats. *Int. J. Pharm.* 513, 78-
 611 87.

612 Nielsen, C.U., Amstrup, J., Steffansen, B., Frokjaer, S., Brodin, B., 2001. Epidermal growth factor inhibits
613 glycylsarcosine transport and hPepT1 expression in a human intestinal cell line. *Am. J. Physiol. Gastrointest.*
614 *Liver Physiol.* 281, 191-199.

615 Nielsen, R.B., Nielsen, U.G., Holm, R., Nielsen, C.U., 2020. Zosuquidar alters etoposide permeability across
616 Caco-2 cell monolayers by P-glycoprotein inhibition in a concentration-dependent manner.
617 https://nordicpop.ku.dk/documents/Booklet_final.pdf, page 30. (accessed 27.04.2020).

618 Palmeira, A., Sousa, E., H Vasconcelos, M., M Pinto, M., 2012. Three decades of P-gp inhibitors: skimming
619 through several generations and scaffolds. *Curr. Med. Chem.* 19, 1946-2025.

620 Prudic, A., Kleetz, T., Korf, M., Ji, Y., Sadowski, G., 2014. Influence of copolymer composition on the
621 phase behavior of solid dispersions. *Mol. Pharm.* 11, 4189-4198.

622 Sezgin, Z., Yuksel, N., Baykara, T., 2007. Investigation of pluronic and PEG-PE micelles as carriers of
623 meso-tetraphenyl porphine for oral administration. *Int. J. Pharm.* 332, 161-167.

624 Shaik, N., Pan, G., Elmquist, W.F., 2008. Interactions of pluronic block copolymers on P-gp efflux activity:
625 Experience with HIV-1 protease inhibitors. *J. Pharm. Sci.* 97, 5421-5433.

626 Shirasaka, Y., Kuraoka, E., Spahn-Langguth, H., Nakanishi, T., Langguth, P., Tamai, I.J.J.o.P., Therapeutics,
627 E., 2010. Species difference in the effect of grapefruit juice on intestinal absorption of talinolol between
628 human and rat. *J. Pharmacol. Exp. Ther.* 332, 181-189.

629 Siegers, C.-P., Strubelt, O., Back, G.J.E.j.o.p., 1972. Inhibition by caffeine of ethanol absorption in rats. *Eur.*
630 *J. Pharmacol.* 20, 181-187.

631 Sparreboom, A., Asperen, J.V., Mayer, U., Schinkel, A.H., Smit, J.W., Dirk, K.F.M., Borst, P., Nooijen,
632 W.J., Beijnen, J.H., Tellingen, O.V., 1997. Limited Oral Bioavailability and Active Epithelial Excretion of
633 Paclitaxel (Taxol) Caused by P-glycoprotein in the Intestine. *Proc. Natl. Acad. Sci. U. S. A.* 94, 2031-2035.

634 Terao, T., Hisanaga, E., Sai, Y., Tamai, I., Tsuji, A., 1996. Active Secretion of Drugs from the Small
635 Intestinal Epithelium in Rats by P-Glycoprotein Functioning as an Absorption Barrier. *J. Pharm. Pharmacol.*
636 48, 1083-1089.

637 Troutman, M.D., Thakker, D.R., 2003a. Efflux Ratio Cannot Assess P-Glycoprotein-Mediated Attenuation
638 of Absorptive Transport: Asymmetric Effect of P-Glycoprotein on Absorptive and Secretory Transport
639 Across Caco-2 Cell Monolayers. *Pharm. Res.* 20, 1200-1209.

640 Troutman, M.D., Thakker, D.R., 2003b. Rhodamine 123 Requires Carrier-Mediated Influx for Its Activity as
641 a P-Glycoprotein Substrate in Caco-2 Cells. *Pharm. Res.* 20, 1192-1199.

642 Tsuruo, T., Tsuruo, T., Iida, H., Iida, H., Tsukagoshi, S., Tsukagoshi, S., Sakurai, Y., Sakurai, Y., 1981.
643 Overcoming of vincristine resistance in P388 leukemia in vivo and in vitro through enhanced cytotoxicity of
644 vincristine and vinblastine by verapamil. *Cancer Res.* 41, 1967-1972.

645 vanAsperen, J., vanTellingen, O., Sparreboom, A., Schinkel, A.H., Borst, P., Nooijen, W.J., Beijnen, J.H.,
646 1997. Enhanced oral bioavailability of paclitaxel in mice treated with the P-glycoprotein blocker SDZ PSC
647 833. *Br. J. Cancer* 76, 1181-1183.

648 Varma, M.V.S., Ashokraj, Y., Dey, C.S., Panchagnula, R., 2003. P-glycoprotein inhibitors and their
649 screening: a perspective from bioavailability enhancement. *Pharmacol. Res.* 48, 347-359.

650 Varma, M.V.S., Panchagnula, R., 2005. Enhanced oral paclitaxel absorption with vitamin E-TPGS: Effect on
651 solubility and permeability in vitro, in situ and in vivo. *Eur. J. Pharm. Sci.* 25, 445-453.

652 Wan, D.-H., Zheng, O., Zhou, Y., Wu, L.-Y., 2010. Solubilization of Ibuprofen in Pluronic Block
653 Copolymer F127 Micelles. *Acta Physico-Chimica Sinica* 26, 3243-3248.

654 Wang, E.-j., Casciano, C.N., Clement, R.P., Johnson, W.W., 2001. HMG-CoA Reductase Inhibitors (Statins)
655 Characterized as Direct Inhibitors of P-Glycoprotein. *Pharm. Res.* 18, 800-806.

656 Wei, Z., Yuan, S., Hao, J., Fang, X., 2013. Mechanism of inhibition of P-glycoprotein mediated efflux by
657 Pluronic P123/F127 block copolymers: Relationship between copolymer concentration and inhibitory
658 activity. *Eur. J. Pharm. Biopharm.* 83, 266-274.

659 Xu, S., Dai, W.-G., 2013. Drug precipitation inhibitors in supersaturable formulations. *Int. J. Pharm.* 453, 36-
660 43.

661 Zamek-Gliszczynski, M.J., Bedwell, D.W., Bao, J.Q., Higgins, J.W., 2012. Characterization of SAGE Mdr1a
662 (P-gp), Bcrp, and Mrp2 knockout rats using loperamide, paclitaxel, sulfasalazine, and
663 carboxydichlorofluorescein pharmacokinetics. *Drug Metab. Dispos., dmd.* 112.046508.

664 Zhang, H., Yao, M., Morrison, R.A., Chong, S., 2003. Commonly used surfactant, Tween 80, improves
665 absorption of P-glycoprotein substrate, digoxin, in rats. *Arch. Pharm. Res.* 26, 768-772.

666 Zhao, G., Huang, J., Xue, K., Si, L., Li, G., 2013. Enhanced intestinal absorption of etoposide by self-
667 microemulsifying drug delivery systems: Roles of P-glycoprotein and cytochrome P450 3A inhibition. *Eur.*
668 *J. Pharm. Sci.* 50, 429-439.

669 Zhao, W., Uehera, S., Tanaka, K., Tadokoro, S., Kusamori, K., Katsumi, H., Sakane, T., Yamamoto, A.,
670 2016. Effects of Polyoxyethylene Alkyl Ethers on the Intestinal Transport and Absorption of Rhodamine
671 123: A P-glycoprotein Substrate by In Vitro and In Vivo Studies. *J. Pharm. Sci.* 105, 1526-1534.

672

673 **Figures Legends:**

674 **Figure 1. Transepithelial P-gp dependent flux of etoposide across Caco-2 cell monolayers.** The
675 steady-state P-gp dependent flux ($\text{pmol cm}^{-2} \text{ min}^{-1}$) of etoposide across Caco-2 cells grown on
676 permeable support for 24-28 days was studied as a function of etoposide concentration (C_d , μM) in
677 the donor solution. The A-B transport (**A**) and B-A (**B**) transport was measured in 3 cell passages. In

678 B, the line is obtained by fitting experimental points to Eq. 1 described in Materials and Methods.
679 Values are given as mean \pm SEM.

680

681 **Figure 2. Pictures of etoposide formulations after 15 hours of storage at room temperature.**

682 Formulation B contained 12 mg mL⁻¹ etoposide, 10% (w/v) of pluronic[®] F-127 in 44% (v/v) ethanol.

683 Formulation G contained 16 mg mL⁻¹ etoposide, 10% (w/v) of pluronic[®] F-127, and 10% (w/v) of

684 PVP/VA in 57% (v/v) ethanol.

685

686 **Figure 3. Absorbance measurements at 400 nm of etoposide formulations added to fasted state**
687 **simulated intestinal fluid (FaSSIF) in a ratio of (Formulation:FaSSIF, 1:2) as a function of time.**

688 Etoposide formulations were composed as shown in Table 1. The measurements were performed at
689 room temperature. For formulation G, n=4 and as mean \pm SEM, for other formulations n=1.

690

691 **Figure 4. Time dependent release of etoposide and glycine from different formulations across**

692 **0.03 μ m polycarbonate membrane.** Donor solutions of ³H-etoposide and ¹⁴C-glycine were prepared

693 in Hanks Balanced Salt Solution (HBSS) buffer supplemented with 10 mM HEPES and adjusted to

694 pH 7.40 \pm 0.05 (Control), or in different formulation-matrix containing 10% (w/v) PVP/VA, 57%

695 (v/v) ethanol, and pluronic[®] F-127 (PF127) at 1.5, 3, or 10% (w/v), referred as Matrix-PF127 1.5%,

696 Matrix-PF127 3%, or Matrix-PF127 10%, respectively, or mixed with formulation G which contained

697 15-16 mg mL⁻¹ etoposide, 10% (w/v) of PF127 and PVP/VA, and 57% (v/v) ethanol. Receiver-release

698 media were HBSS buffer supplemented with 10 mM HEPES and adjusted to pH 6.50 \pm 0.05 for all

699 conditions, except in formulation G condition where the receiver-release media was the matrix of

700 formulation G (i.e. 10% (w/v) of PF127 and PVP/VA, and 57% ethanol, and q.s. water but without
701 etoposide). Experiments were performed at 37 °C and shaking mode 220 rpm. Data are expressed in
702 mean \pm SEM from 3-4 independent membranes and as one membrane per experiment.

703

704

705 **Figure 5. Plasma concentration time profile of etoposide after intravenous administration of 5**
706 **mg kg⁻¹ etoposide to wild-type male Sprague-Dawley rats.** Each data point is shown as mean \pm
707 SEM from 3-6 rats.

708

709 **Figure 6. Plasma concentration time profiles of etoposide after oral administration of different**
710 **doses of etoposide in wild-type male Sprague-Dawley rats.** A) Etoposide was administered orally
711 at a dose of 20 mg kg⁻¹ in 57% (v/v) ethanol solution (Control), or at increasing doses of etoposide
712 dissolved in matrix at 20, 50, and 100 mg kg⁻¹ etoposide. The matrix was consisted of 10 % (w/v)
713 pluronic[®] F-127 and PVP/VA, and 57% (v/v) ethanol, and q.s. water. At the highest oral dose, the
714 formulation is referred as formulation G. B) Etoposide was administered orally as control after the
715 rats were received an oral dose 20 mg kg⁻¹ of zosuquidar. Each data point is shown as mean \pm SEM
716 from 5-6 rats. The solid lines are only connecting the data points.

717

718 **Supplementary Figure S1. AUC after oral administration as a function of dose.**

719 Each data point is shown as mean \pm SEM from 5-6 rats.

720

Table 1: Composition of oral formulations of etoposide. (nd : not determined, ✓: Yes, ÷ : no).

^a: (Li et al., 2012; Xu and Dai, 2013)

	Formulations							Function
	A	B	C	D	E	F	G	
Composition								
Etoposide (mg mL⁻¹)	9	12	12	15	15	15	16	API, P-gp substrate
Pluronic® F-127 (% w/v)	4.7	10	6	6	2	6	10	Surfactant, precipitation inhibitor ^a
PVP/VA (% w/v)	5	-	15	-	5	10	10	Precipitation inhibitor
Ethanol (% v/v)	44	44	57	57	57	57	57	Co-solvent/solvent
Ultra-purified water	qs	qs	qs	qs	qs	qs	Qs	Solvent
Stable under storage for 15 h	✓	÷	✓	✓	✓	✓	✓	
Stable for 2 h after dilution with FaSSIF	nd	nd	÷	÷	÷	÷	✓	

Table 2: Population pharmacokinetic parameter estimates of the base structural model and the final covariate model. Precision of the parameter estimates is reported as relative standard error (RSE%). F = oral bioavailability, k_a = absorption rate, V1 = volume of the central compartment, V2 = volume of the peripheral compartment, CL = elimination clearance, Q2 = intercompartmental clearance, $\beta_{F,FORM}$ = categorical covariate effect of formulation G presence on F, $\beta_{F,ZOSU}$ = categorical covariate effect of zosuquidar presence on F, $\beta_{k_a,FORM}$ = categorical covariate effect of formulation G presence on k_a , a = additive error model term, b = proportional error model term, OFV = objective function value, -2LL = minus 2 times log likelihood, AIC = Akaike information criterion.

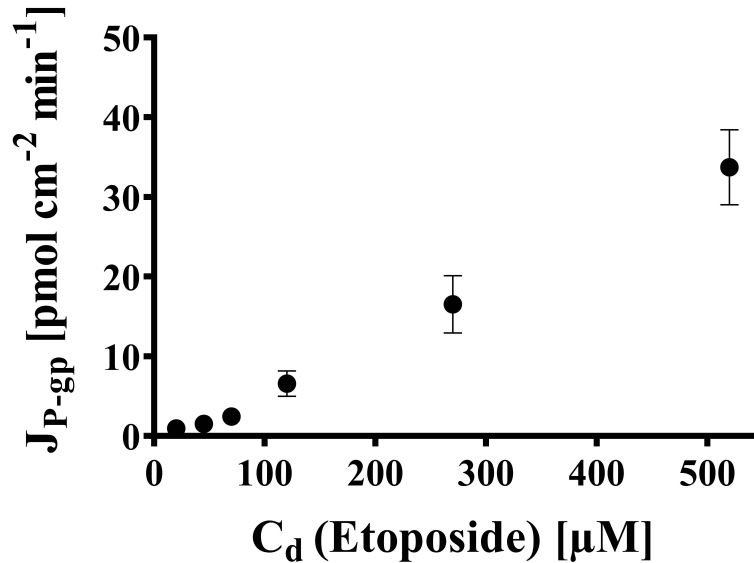
	Base structural model	Final covariate model
Fixed effects [RSE%]		
F (%)	6.76 [24.2]	3.92 [16.7]
k_a (h⁻¹)	2.69 [13.1]	4.54 [20.2]
V1 (L kg⁻¹)	3.63 [18]	2.91 [18.7]
V2 (L kg⁻¹)	3.18 [12.2]	3.78 [17.9]
CL (L h⁻¹ kg⁻¹)	1.61 [4.62]	1.55 [10.1]
Q2 (L h⁻¹ kg⁻¹)	6.56 [13.6]	6.98 [18.6]
$\beta_{F,FORM}$	-	-0.51 [37.9]
$\beta_{F,ZOSU}$	-	2.17 [7.04]
$\beta_{k_a,FORM}$	-	-0.713 [34.8]
Random effects (SD) [RSE%]		
F	1.1 [13.4]	0.158 [28.1]
k_a	0.552 [20.6]	0.502 [23.2]
V1	0.924 [13]	0.678 [15]
CL	0.122 [35.6]	0.118 [38.8]
Error model [RSE%]		
a	0.01 [14.1]	0.0115 [14.5]
b	0.132 [9.34]	0.135 [10.9]
OFV		
-2LL	-665.17	-734.78
AIC	-641.17	-704.78

Table 3: Estimated pharmacokinetic parameters after intravenous and oral administration of different doses of etoposide in wild-type male Sprague-Dawley rats. Matrix solution consisted of 10 % (w/v) pluronic[®] F-127, 10% (w/v) PVP/VA, 57% (v/v) ethanol, and q.s. water. Individual Bayesian (post hoc) estimates were used to calculate mean AUC_{0-∞}. Data are expressed as mean ± SEM except for t_{max} that is expressed as the median [Q1; Q3] (25% and 75% percentile). No random effects were estimated for Q and V₂. Fixed effects were estimated as Q = 6.98 mL h⁻¹ kg⁻¹, V₂ = 3778 mL kg⁻¹. Statistical significance was tested by one-way ANOVA followed by Tukey's multiple comparisons test. When all the groups, except the group of rats pre-dosed with zosuquidar and the group of rats receiving i.v. administration, were included in the comparison, (*) referred to P < 0.05 compared to control. When all the groups, except the group of rats receiving i.v. administration, were included in the comparison, (†) referred to P < 0.05 compared to control.

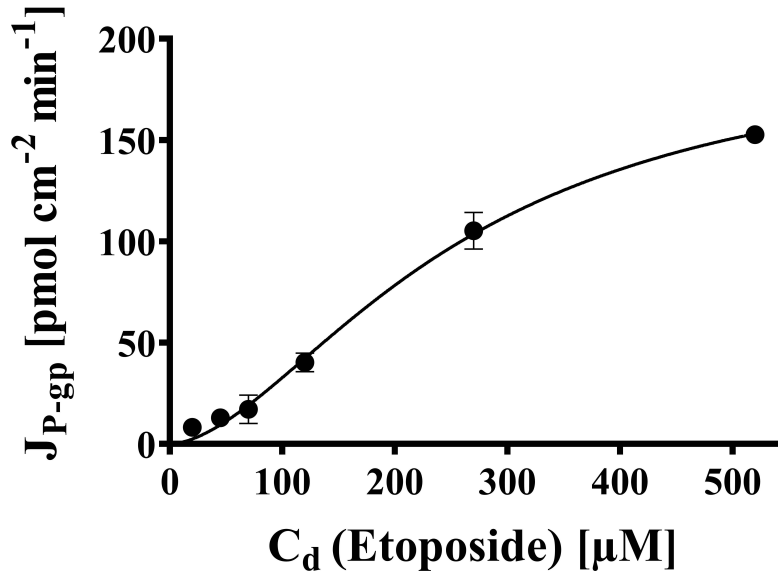
Study cohorts						
Etoposide dose	20 mg kg ⁻¹	20 mg kg ⁻¹	50 mg kg ⁻¹	100 mg kg ⁻¹	20 mg kg ⁻¹	5 mg kg ⁻¹
Condition	Control				Zosuquidar	
Etoposide solution	57% EtOH	Matrix	Matrix	Matrix	57% EtOH	57% EtOH
Cohort Size	6	5	6	6	6	6
Administration route	p.o.	p.o.	p.o.	p.o.	p.o.	i.v.
F (%)	4.0 ± 0.13	2.4 ± 0.02*	2.4 ± 0.07*	2.2 ± 0.09*	34.5 ± 0.18 [†]	100 ± 0
k_a (h⁻¹)	6.40 ± 0.94	2.29 ± 0.41* [†]	2.36 ± 0.35* [†]	2.32 ± 0.32* [†]	3.43 ± 0.41 [†]	-

CL (mL h⁻¹ kg⁻¹)	1547 ± 28	1533 ± 6.9	1503 ± 24	1587 ± 39	1550 ± 43	1636 ± 85
V₁ (mL kg⁻¹)	3830 ± 574	4263 ± 193	4143 ± 315	4953 ± 640	2996 ± 436	809 ± 50
AUC_{0-∞} (ng h mL⁻¹)	518.8 ± 25	307.2 ± 3.5*	816.5 ± 38*	1525 ± 86*	4511 ± 384 [†]	3096 ± 155
AUC_{0-∞}/D (h mL⁻¹ kg)	25.9 ± 1.3	15.4 ± 0.2	16.3 ± 0.8	14.2 ± 0.9	225.5 ± 19.2	619.2 ± 31.0
t_{1/2} (h)	1.73 ± 0.27	1.93 ± 0.08	1.91 ± 0.14	2.18 ± 0.31	1.36 ± 0.23	0.35 ± 0.02
t_{max} (h)	0.375 [0.25-0.5]	0.625 [0.44-0.75]	0.75 [0.25-1.06]	0.75 [0.5-1.25]	0.5 [0.5-0.81]	-
C_{max} (ng mL⁻¹)	191 ± 19	63 ± 4*	169 ± 17	266 ± 38*	1542 ± 190 [†]	-

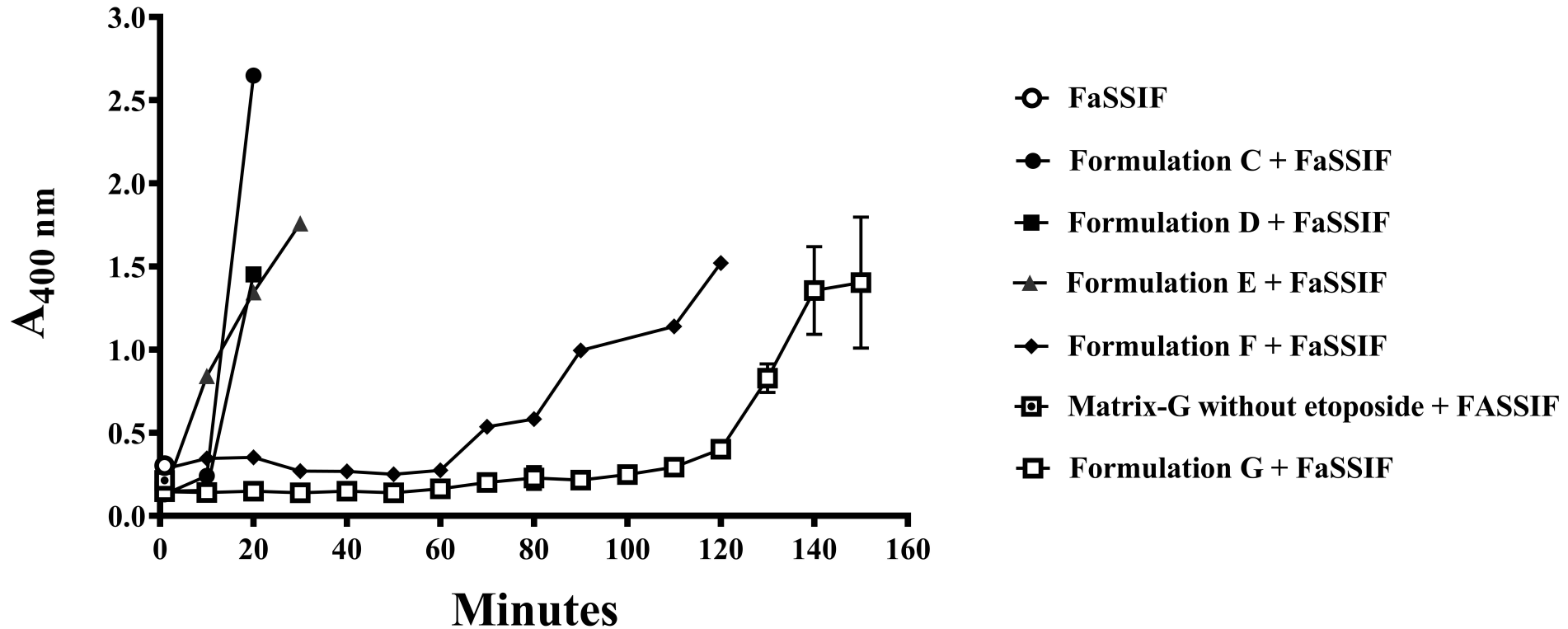
A) A-B



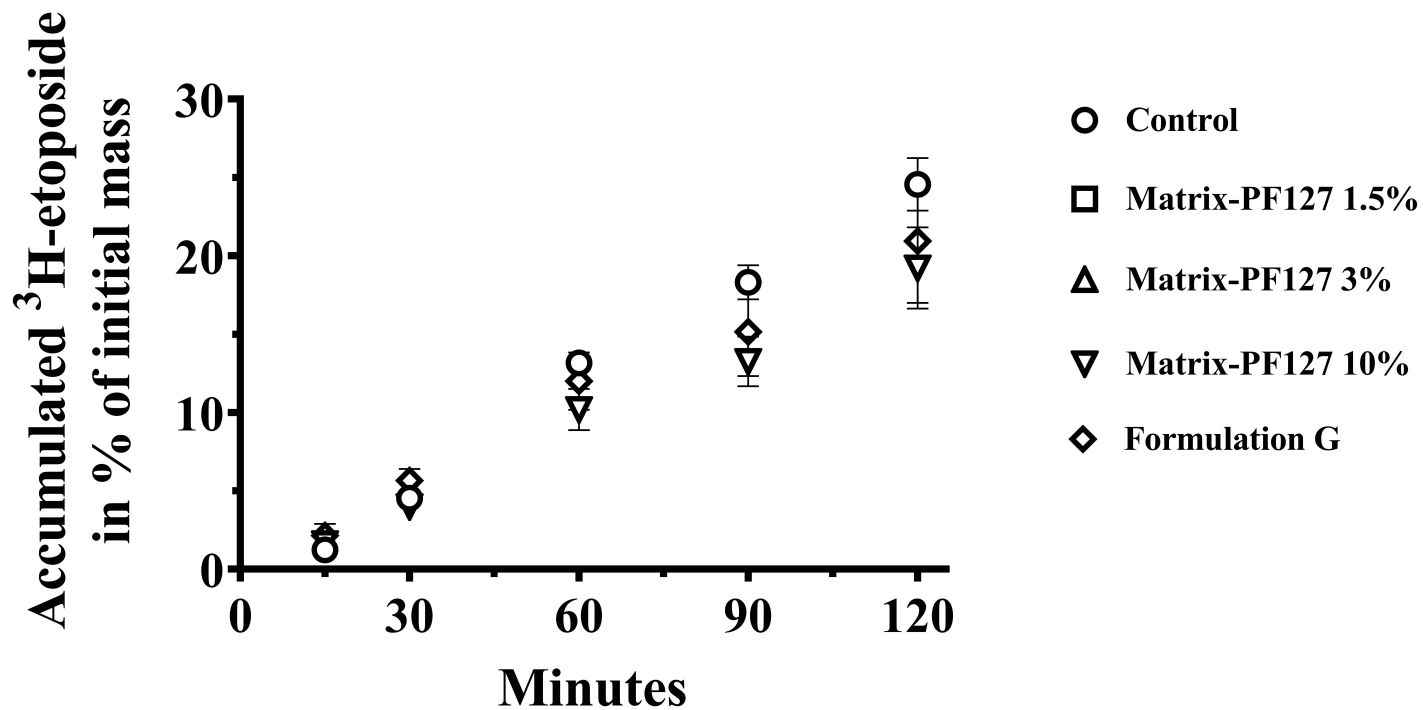
B) B-A



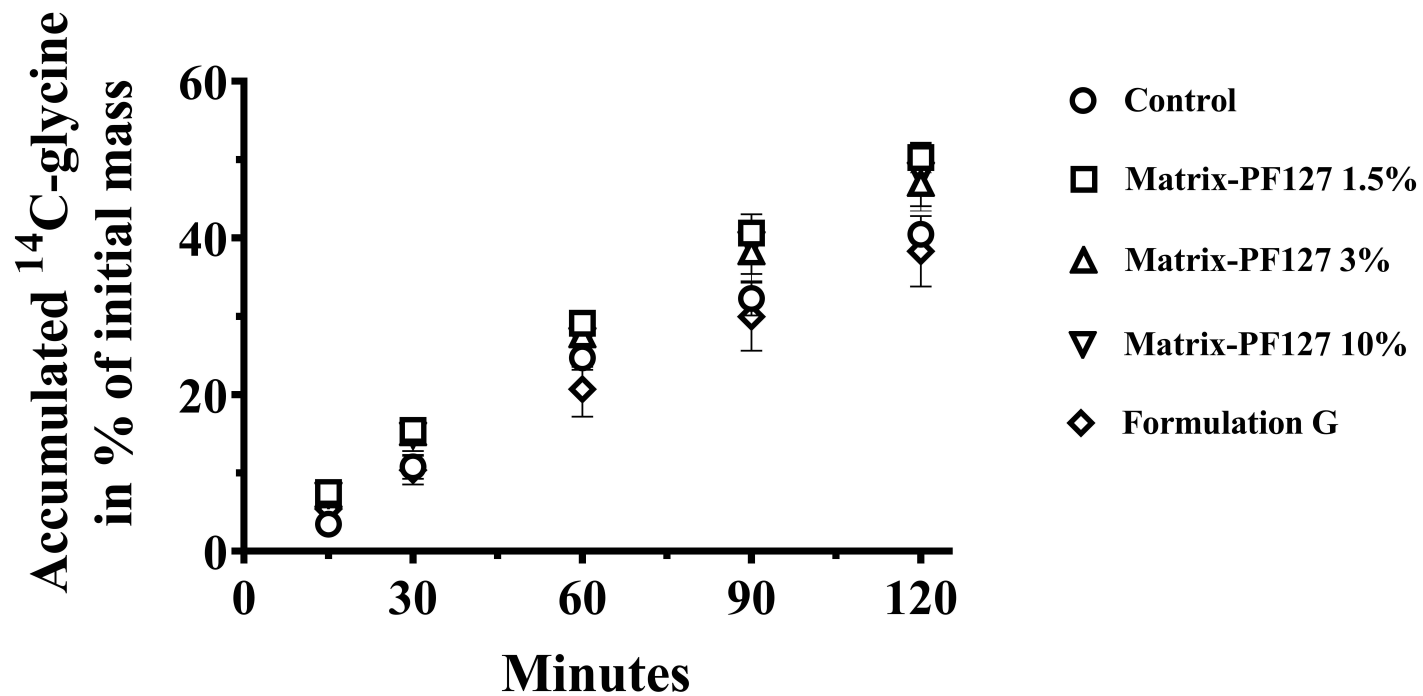


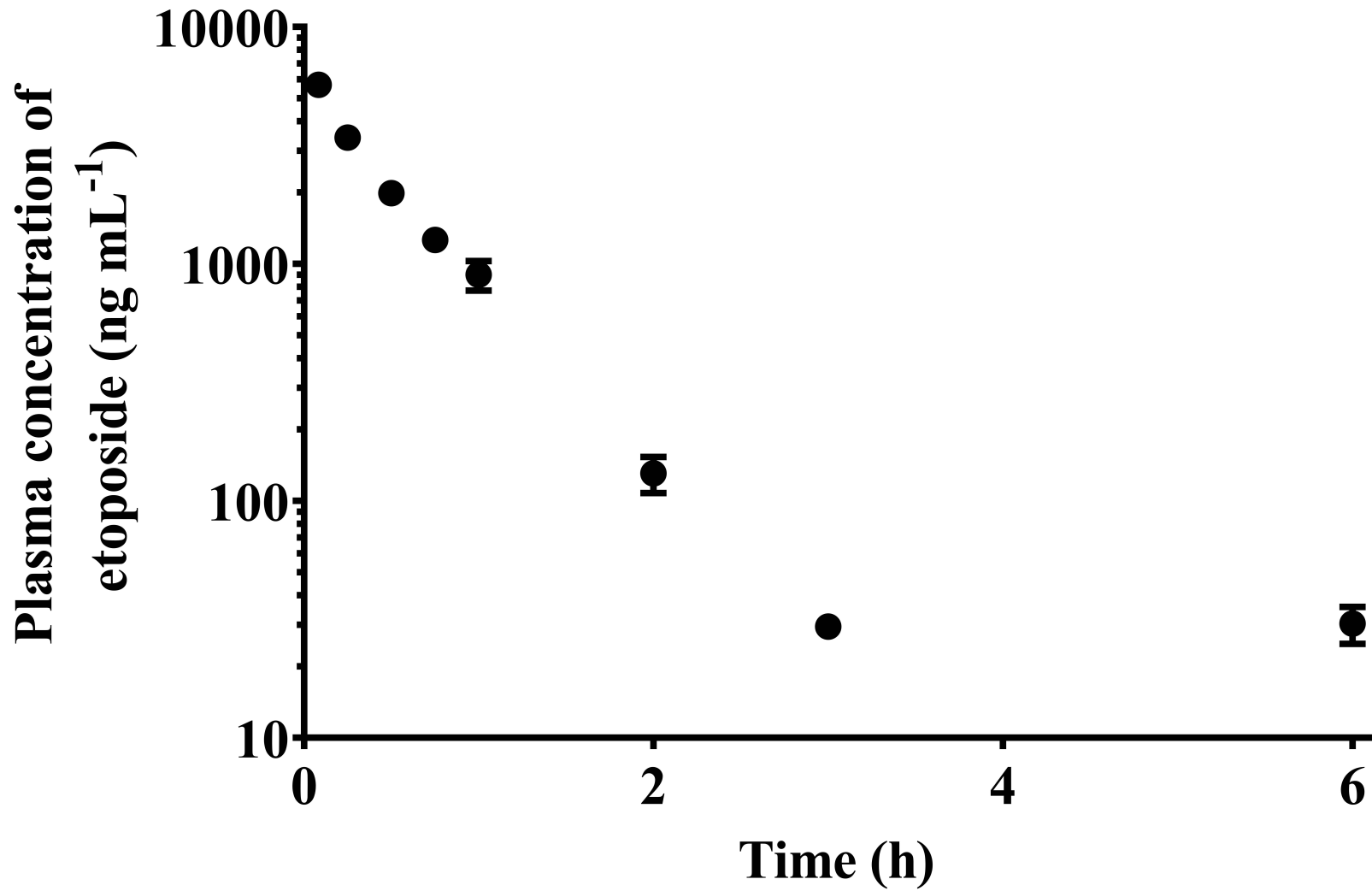


(A)

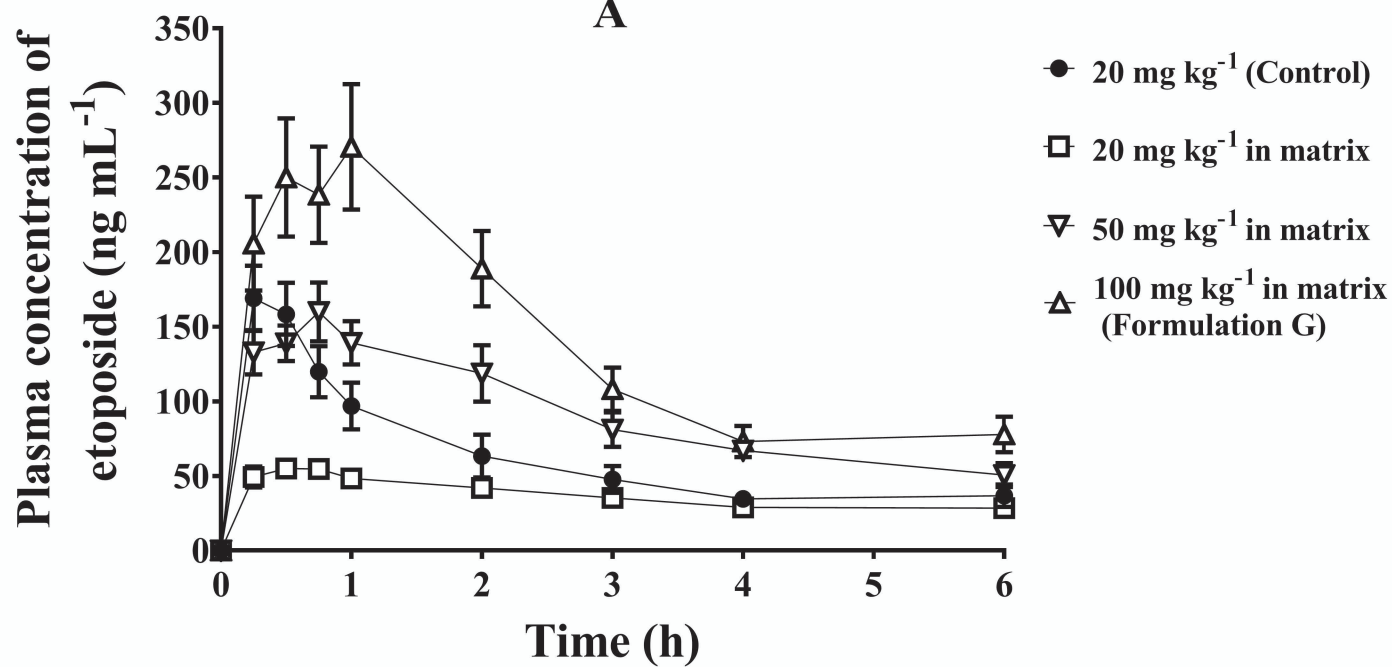


(B)





A



B

